JOURNAL OF MATERIALS SCIENCE 32 (1997) 4117–4126

Weld microstructure refinement in a 1441 grade aluminium–lithium alloy

G. MADHUSUDHAN REDDY, AMOL A. GOKHALE
Defence Metallurgical Research Laboratory, Hyderabad, India 500 058
K. PRASAD RAO
Department of Metallurgical Engineering, Indian Institute of Technology, Madras, India

Clad 2 mm thick sheets of Russian 1441 grade Al–Li alloys were welded using a gas tungsten arc welding process (GTAW). Comparisons were made between the weld beads obtained under (i) continuous current (CC), (ii) pulsed current (PC), and (iii) arc oscillation (AO) conditions for their macro- and microstructural details. In the case of CC GTAW, sound welds could be produced only under a narrow range of welding parameters. Centre line cracks, which occurred in CC GTAW welds under certain conditions, were halted by switching to PC or AO conditions while the welding was in progress. Microstructural refinement was significant in the case of PC and AO GTA welding.

1. Introduction

Aluminium–lithium alloys of different grades have been developed as lower density higher modulus alternatives to other aeronautical grade Al alloys. Russian grade 1441 alloy sheet products, developed around 1987, have the advantages of reduced in-plane property anisotropy and relative insensitivity of fatigue crack growth resistance to sheet thickness [1].

Weldability of Al–Li based alloys has been discussed in detail in a review by Pickens [2]. Studies on the effects of welding conditions on weld soundness and macro/microstructure in 8090 type alloys have also been reported [3, 4]. Aluminium alloys welded under conventional (continuous current) GTA welding processes are known to exhibit epitaxial growth from the fusion line leading to a columnar grain structure [5]. It is, however, desirable to have a fine equiaxed grain structure to reduce hot cracking [6], weld porosity and segregation [7], and to improve weld toughness. Several attempts have been made on some aluminium alloys and other alloys to refine the bead microstructure using techniques like inoculation [8, 9], electrode vibration [10], current pulsation [11, 12] and arc oscillation [12–14]. However, no such attempts have been reported in the case of Al–Li alloys.

In the current study, an experimental work has been taken up on the alloy 1441 to evaluate the effects of two variations in the conventional continuous current (CC) GTA welding process, namely pulsed current (PC) and arc oscillation (AO). The influence of welding methods on centre line cracking, and the morphology and scale of the bead solidification structure have been studied. New evidence on the existence of a "chill zone" near the fusion line is also reported.

2. Experimental procedure

Aluminium–lithium alloy 1441 was made in the form of 2 mm thick rolled sheets under a joint Indo–Russian programme. The chemical composition of the alloy is given in Table I. The alloy sheets were clad 2–4% of the sheet thickness on each side by AA 7072 alloy. The sheets were heat-treated to the T81 temper, i.e. solution treated, 2% cold stretched and aged at 170 °C for 24 h prior to welding. Coupons of 250×100 mm size were cut such that the coupon length was parallel to the rolling direction. Bead-on-plate welds were made without a filler metal perpendicular to the rolling direction by the alternating current (a.c.) GTA welding process. Weld coupons were clamped in a jig with the joint line held over a channel that could be purged with backing argon gas, as shown in Fig. 1. Welds were made with two variations in the conventional (CC) GTA welding process, namely pulsed current (PC) GTA welding and GTA welding with magnetically induced arc oscillation (AO). The direction of arc oscillation was transverse to the welding direction. Weld surfaces were prepared prior to welding, the details of which can be found in [3]. Weld parameters chosen were those that gave sound welds with full penetration, and are listed in Table II.

The weld bead macro- and microstructures were studied by metallography of various sections prepared by the standard polishing techniques used for aluminium alloys and etched using Keller's reagent. Elemental segregation in the weld zone was revealed by X-ray mapping for the individual elements using the electron probe microanalyser (EPMA). Tensile fracture surfaces and weld crack surfaces were observed using the secondary electron images on the scanning electron microscope (SEM). Tensile tests

0022–2461

were performed on an Instron 1185 universal testing machine using flat tensile test pieces conforming to ASTM E8 (25 mm GL) standard. The crosshead speed during the tensile tests was maintained at 1 mm min^{-1}. The elongation values were calculated based on the extensometer gauge length, although the strain was likely to be concentrated in the weld bead area.

3. Results

3.1. Macrostructure

The macrostructure of the weld beads under the three types of arc conditions is shown in Fig. 2. The structure consisted of:

(a) a narrow white band at the fusion line (marked 1),
(b) a zone of structure not resolvable at the given magnification (marked 2);
(c) a zone of columnar grains (marked 3); and
(d) a central region of equiaxed grains (marked 4).

It can be seen that in the case of continuous current welding, the columnar grains extended up to the weld centre line, while equiaxed grains formed in the region near the weld centre line in PC and AO welds.

3.2. Microstructure

The microstructure within the various zones of the weld (reported in the previous section) will be described next. Zone 1 of Fig. 2 consisted of partially melted grains in all types of welds and is marked as PMZ in Figures 3, 4 and 5. The partially melted grains are roughly of the same size as the heat affected zone HAZ grains. A globular phase is seen within the grains in this region.

The next adjacent zone into the weld bead, i.e. zone 2 of Fig. 2, consists of fine cells and is similar in appearance to a "chill zone" in castings (see Figs 3–5). The "chill" zone shown here has much finer grain size than the base metal and, therefore, is distinct from the zone of partially melted grains. The "chill zone" also manifests itself as bands in PC welds (Figs 4 and 6) because a PC weld consists of a series of overlapping beads and for every new bead that solidifies, a band of chill grains would be left along the trailing edge of the pool.

The "chill" zone is followed by the columnar dendritic zone (zone 3 of Fig. 2, and marked as "columnar zone" in Figs 3–5) in all cases. The grain aspect ratio

TABLE I Chemical composition of the base alloy (wt %)

Al	Li	Cu	Mg	Zr	Be	Ti	Fe	Si
Balance	1.9	2.0	0.9	0.09	0.05	0.02	0.11	0.05

TABLE II Welding parameters

Common parameters	
Electrode,	W–2% thorium
Arc length, mm	2
Arc voltage, V	18–20
Torch position,	Vertical
Sheilding argon, %	99.9
Flow rate,	35 CFH
Continuous current welding	
Welding current, A	80
Welding speed, mm s^{-1}	7.5
Pulsed current welding	
Peak current (I_p), A	150
Base current (I_b), A	15
Welding speed, mm s^{-1}	3.4
Pulse duration, %	20
Pulse frequency, Hz	2
Arc oscillation	
Welding current, A	80
Welding speed, mm s^{-1}	5.5
Oscillation frequency, Hz	50
Oscillation amplitude, mm	1

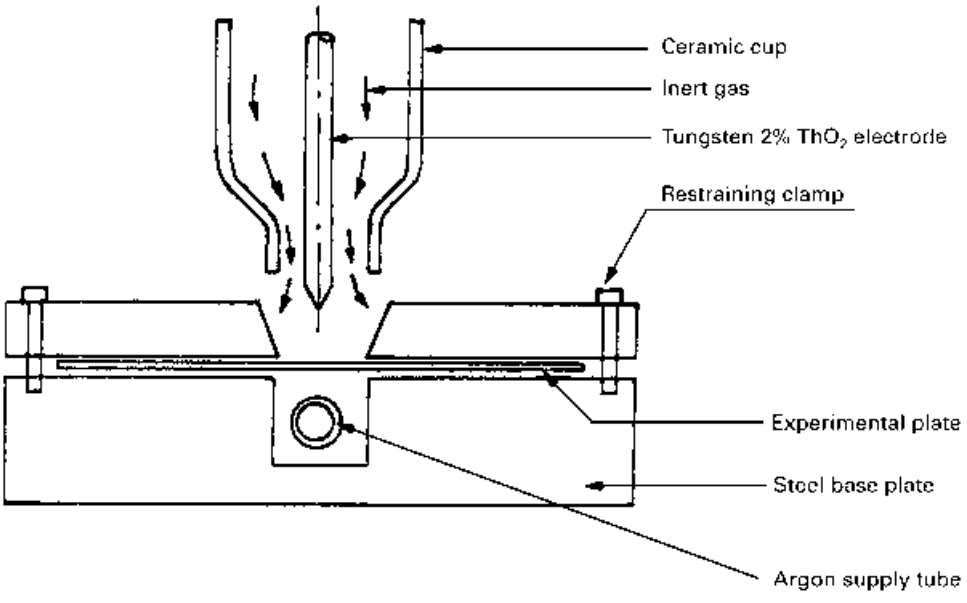

Figure 1 The welding set up.

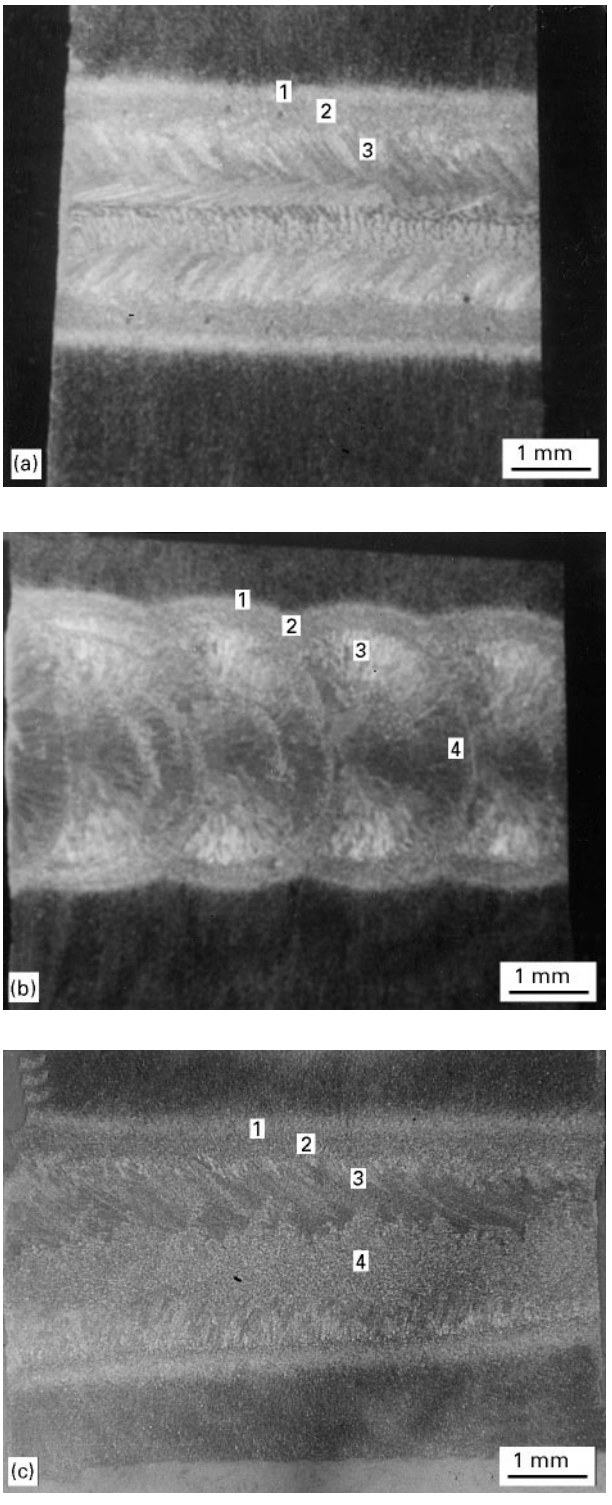

Figure 2 Weld bead macrostructures in 1441 Al–Li alloy: (a) continuous current weld, (b) pulsed current weld, and (c) are oscillation weld.

(dendrite length : width ratio) is highest in the CC welds, medium in the PC welds and lowest in the welds made under AO conditions. Zone 4 of Fig. 2b and c was revealed to have equiaxed grain structure (see Figs 4 and 5). As reported in the previous section, this zone of equiaxed grain structure was not present in CC welds.

Because weld pools have curved boundaries, and the heat input is from a point-like source (the arc), the solid–liquid interface is always curved and the direction of the maximum thermal gradient, G_L, at the solid–liquid interface changes with time. Consequently, the orientations of the columnar grains change with the progress of solidification. This necessitates microstructural observations on additional sections of the weld bead in order to study the grain morphologies. Therefore, weld bead microstructures along the cross-sectional planes were also studied (Figs 6–8). These microstructures contained all the types of grain structures revealed by the top sections of the welds. Also the existence of a "chill zone" near the fusion line was confirmed, although the extent of the zone appeared to be different in the two views in case of PC and AO welds. Secondly, it was found that the columnar nature of the grains is better revealed in the top section rather than in the cross-section. Bands of coarse cells were also seen in AO welds in the cross-section (Fig. 8).

Combining the microstructural information from the weld top sections (Figs 3–5) with that from the weld cross-sections (Figs 6–8) it could be seen that the microstructure was refined in PC and AO welds compared with the CC welds. Additionally it was found that AO welds had finer substructures over wider areas of the weld beads than the PC welds (Figs 6 and 8).

Further, electron probe microanalysis revealed the presence of dark intercellular phases rich in Cu and Mg, and also a phase rich in Si scattered at some grain boundary (GB) triple points (Figs 9–11). The presence of Li in these phases could not be confirmed due to low atomic number. It may be noted that with greater structural refinement (CC to PC to AO welds), the intercellular phase became more discontinuous.

3.3. Propensity for hot cracking

The Al–Li alloy 1441 was found to be prone to hot cracking under continuous current GTA welding. A typical centre line crack along with the surface of the crack is shown in Fig. 12. The crack is seen to be interdendritic in nature without any signs of plastic deformation, confirming it to be a solidification crack, i.e. hot crack. Table III gives the range of welding parameters and the corresponding observations regarding the occurrence of hot cracking and weld metal porosity. It is seen that sound welds could be obtained only over a narrow band of welding conditions. The range of parameters over which sound welds could be obtained was wider for PC and AO welds. Effects of weld parameters on weld quality in PC and AO welding is the subject of another study and the results will be published separately.

In another set of experiments, welding was started at a continuous current under which hot cracking took place (welding speed $= 6\,\mathrm{mm\,s^{-1}}$). The hot cracks progressed in the welding direction along interdendritic boundaries. Subsequently, either current pulsation or arc oscillation was suddenly introduced (conditions as in Table II). The change in arc conditions resulted in a transition from columnar grain structure to a band of "chill zone" and subsequently to an equiaxed grain structure, and simultaneously

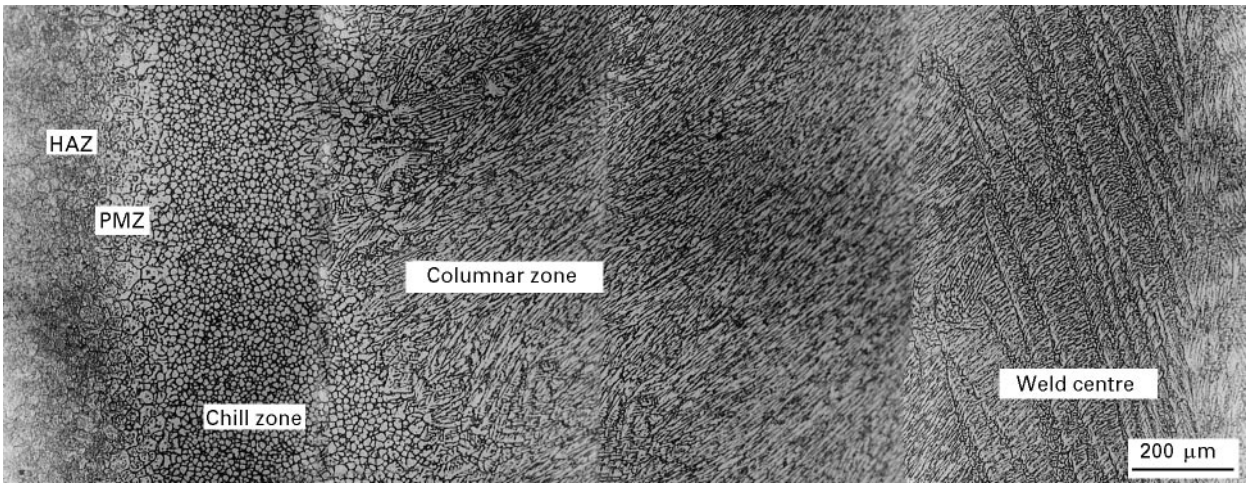

Figure 3 Weld bead microstructure (top section) in a continuous current weld.

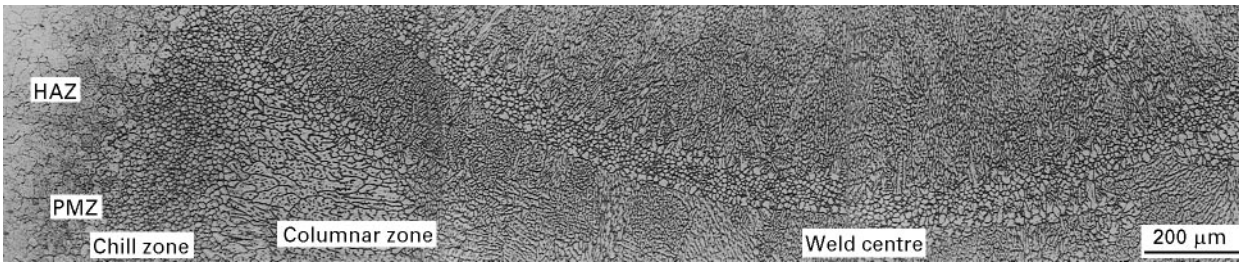

Figure 4 Weld bead microstructure (top section) in a pulsed current weld.

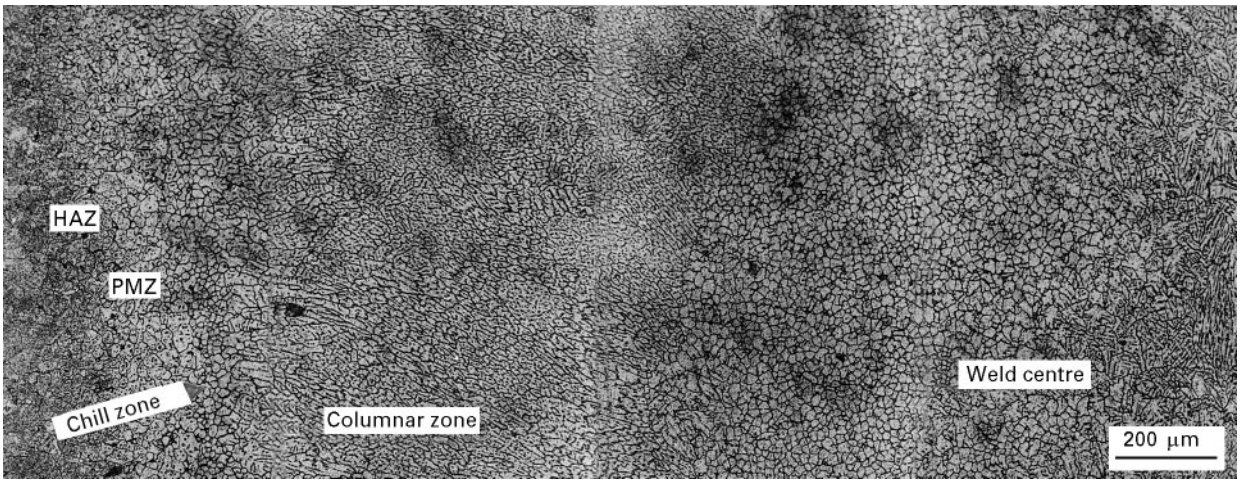

Figure 5 Weld bead microstructure (top section) in an arc oscillation weld.

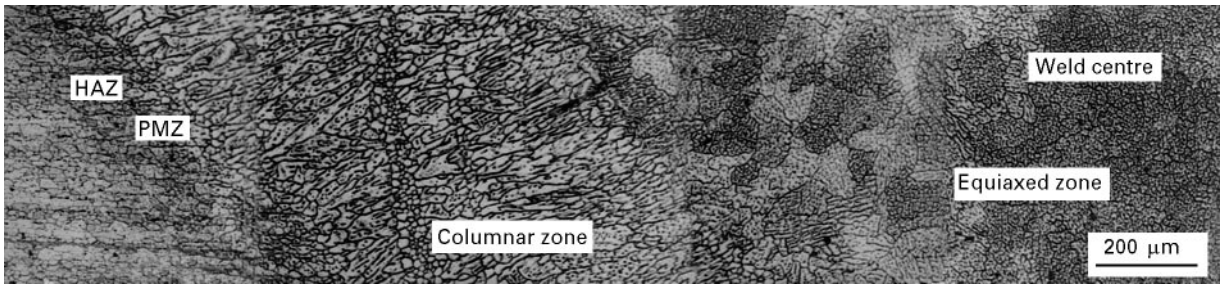

Figure 6 Weld bead microstructure (cross-section) in a pulsed current weld.

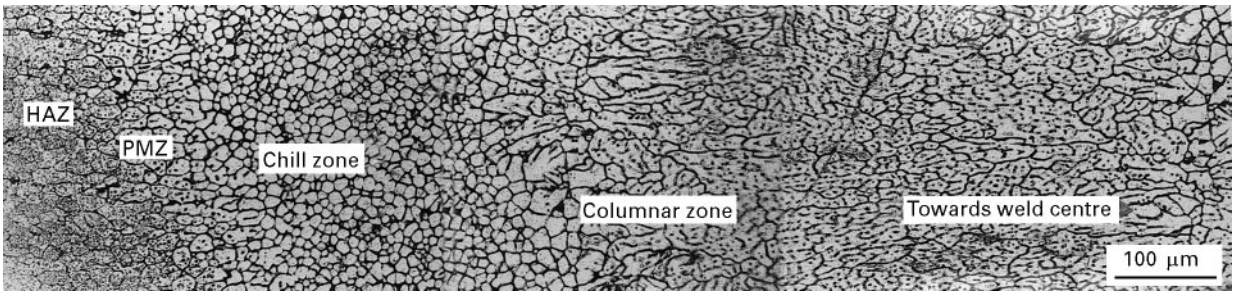

Figure 7 Weld bead microstructure (cross-section) in a continuous current weld.

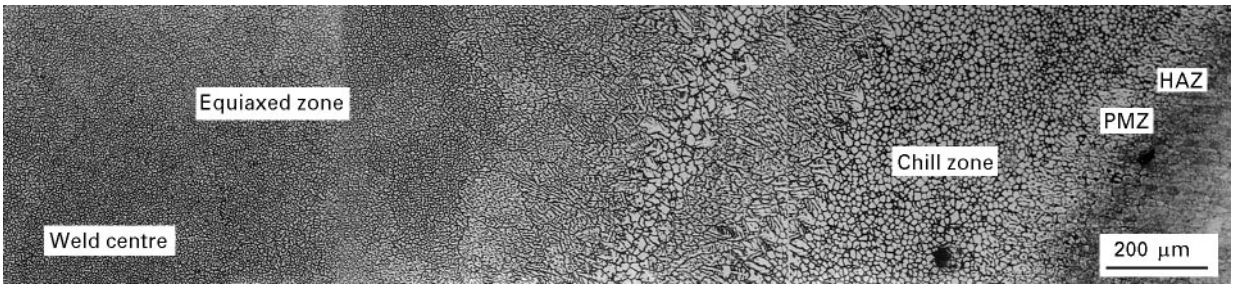

Figure 8 Weld bead microstructure (cross-section) in an arc oscillation weld.

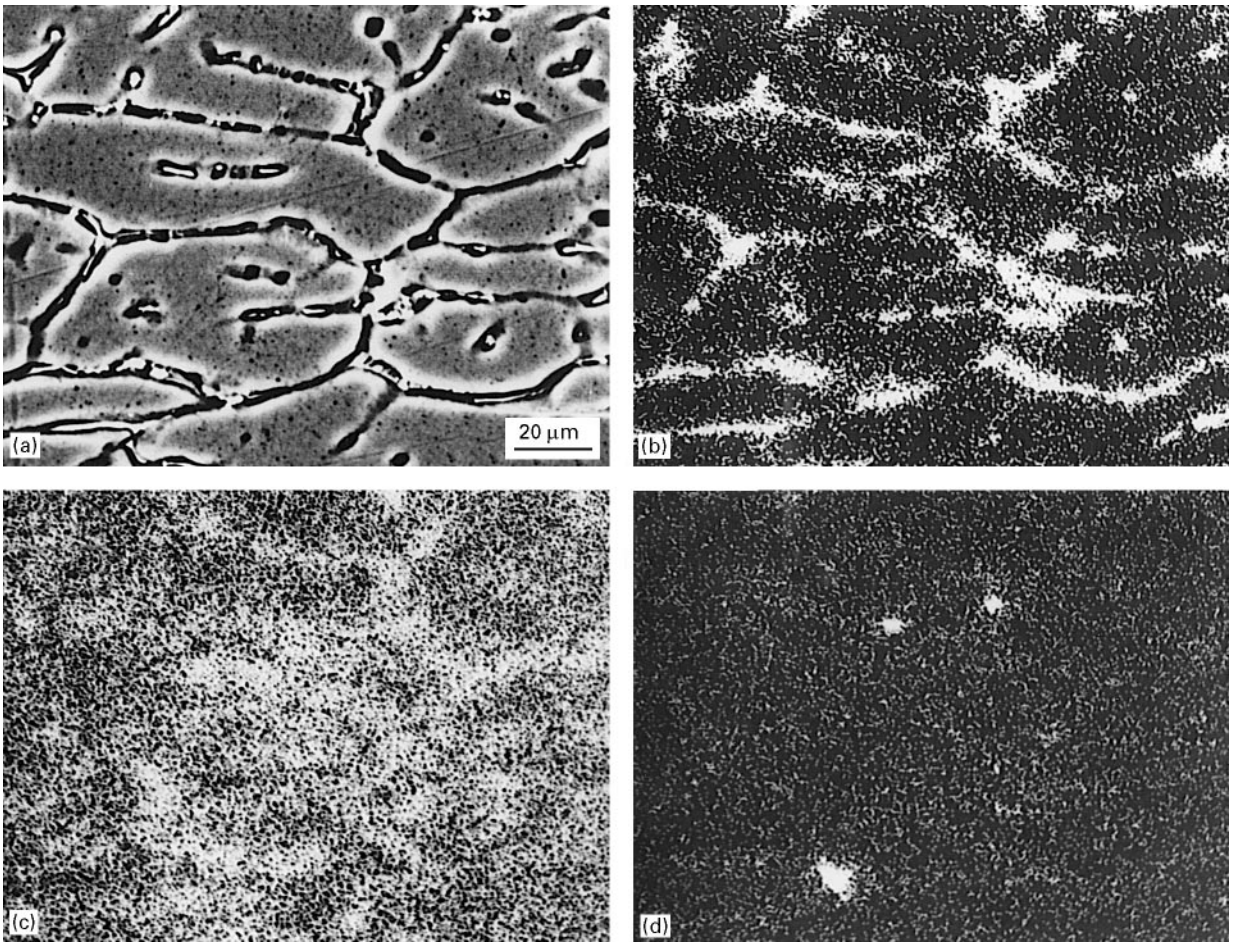

Figure 9 Elemental X-ray maps (EPMA) in a continuous current weld: (a) BSE, (b) Cu, (c) Mg, (d) Si.

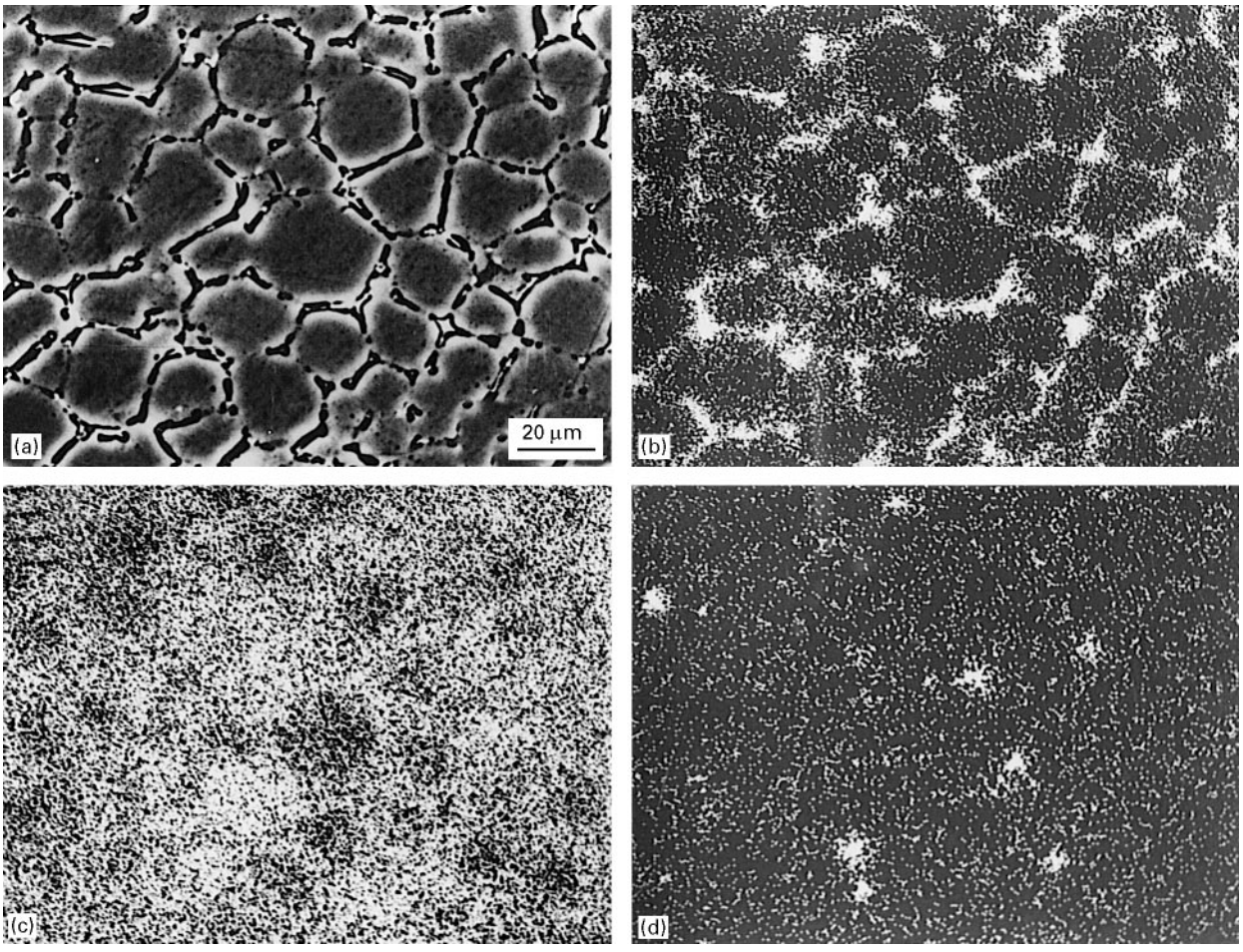

Figure 10 Elemental X-ray maps (EPMA) in a pulsed current weld: (a) BSE, (b) Cu, (c) Mg, (d) Si.

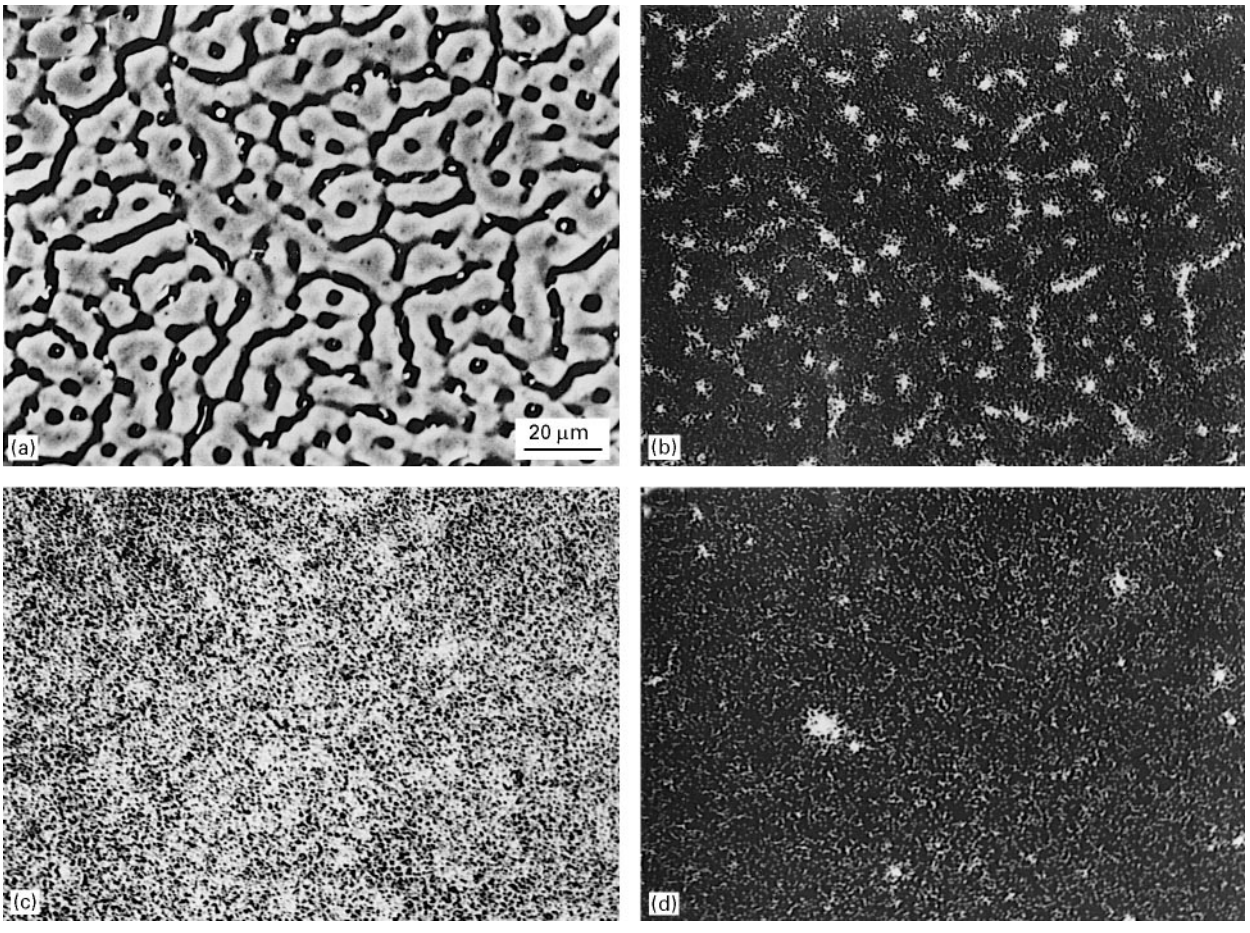

Figure 11 Elemental X-ray maps (EPMA) in an arc oscillation weld: (a) BSE, (b) Cu, (c) Mg, (d) Si.

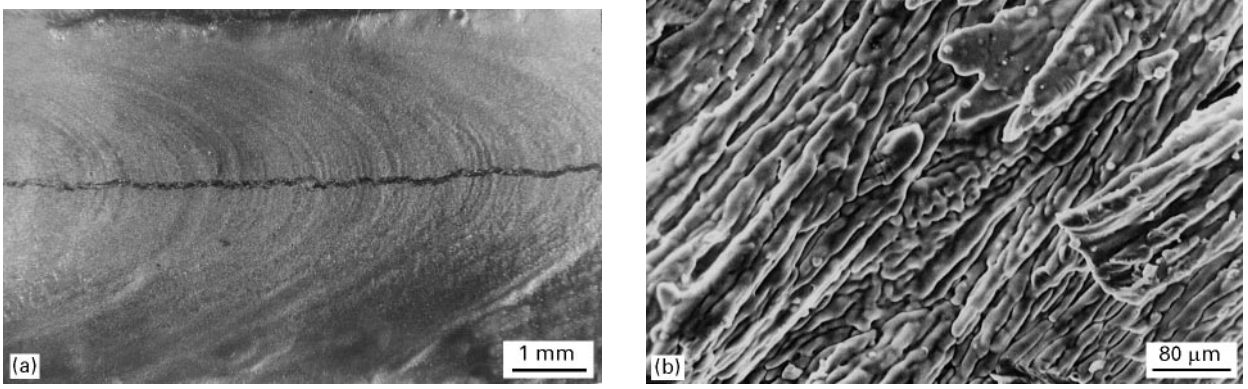

Figure 12 (a) Weld centre line crack in a continuous current weld, (b) crack surface.

TABLE III Observations on weld soundness in continuous current welding of alloy 1441

Sample No.	Current (A)	Voltage (V)	Speed ($mm\,s^{-1}$)	Remarks
1	40	18–20	4.0	Discontinuous cracks in weld centre
2	65	18–20	6.0	Centre line crack observed
3	80	18–20	7.5	Sound weld
4	105	18–20	10.0	Heavy oxidation and porosity, centre line cracking, blow holes
5	120	18–20	12.0	Heavy oxidation and porosity

resulted in crack arrest in both cases, as seen in Fig. 13.

3.4. Tensile properties

Tensile properties were evaluated in the as-welded condition on test coupons cut along the welding direction (all-weld samples), and are presented in Table IV. The yield (YS) and ultimate tensile strengths (UTS) were higher in the case of PC and AO welds compared with CC welds. The ductility in PC and AO welds were significantly improved over that in CC welds. The weld metal efficiency (YS of weld : YS of the base metal) was about 65% in PC welds. The tensile fracture surfaces were highly dimpled in the case of PC and AO welds, but were flatter having coarse, featureless surfaces in CC welds (see Fig. 14). Evaluations of properties across the welding direction and in the heat-treated condition are in progress.

4. Discussion

4.1. Macro- and microstructure

The partially melted zone (PMZ) seen in all the cases described earlier represents the area that experienced temperatures in the solidifcation range of the alloy. The globular phase that is seen within these grains possibly forms as a result of localized melting during welding and subsequent resolidification.

Formation of the columnar zones in all the welds is expected because, in general, the weld pool solidifies under high thermal gradient, G_L, conditions [15]. In CC GTA welding, remelting of heterogeneous nuclei or growth centres (such as broken/remelted dendrites) occurs due to the high temperatures existing in the liquid region. This results in the columnar dendrites growing up to the weld centre line and, therefore, the creation of a plane of weakness.

The existence of a "chill zone" has been revealed earlier in the case of laser glazed Al–Li alloy plates [16]. However, "chill zone" formation in the case of welds has not been shown by earlier investigators for any alloy system. Moreover, the possibility of its formation has been discounted [17] because of epitaxial growth being the predominant mode of solidification near the fusion line. At present, it is not clear why the "chill" zone forms in Al–Li alloys and not in any other alloy system. It appears that some barrier for epitaxial growth must exist that allows undercooling in the fusion zone near the weld pool boundary (where solidification begins) leading to the formation of "chill" crystals. The role of oxidation and surface tension in preventing epitaxial growth needs to be studied further.

The microstructural refinement in PC and AO welds could be considered in the light of the fluid flow and heat transfer conditions expected to prevail during weld pool solidification. In AO welds, for example, the changing location of the heat source in AO welding leads to changes in (a) the arc pressure impingement points and (b) the growth direction of the columnar dendrites. The former phenomenon would be expected to cause greater fluid flow in the weld pool than in the case of CC welding. As a result, the thermal gradient in the liquid ahead of the solid–liquid interface would be reduced thus improving the chances of survival of the heterogeneous nuclei (containing Ti). Also the columnar dendrites, with a zig-zag growth pattern would be more vulnerable to remelting and break-off due to the fluid flow thus generating

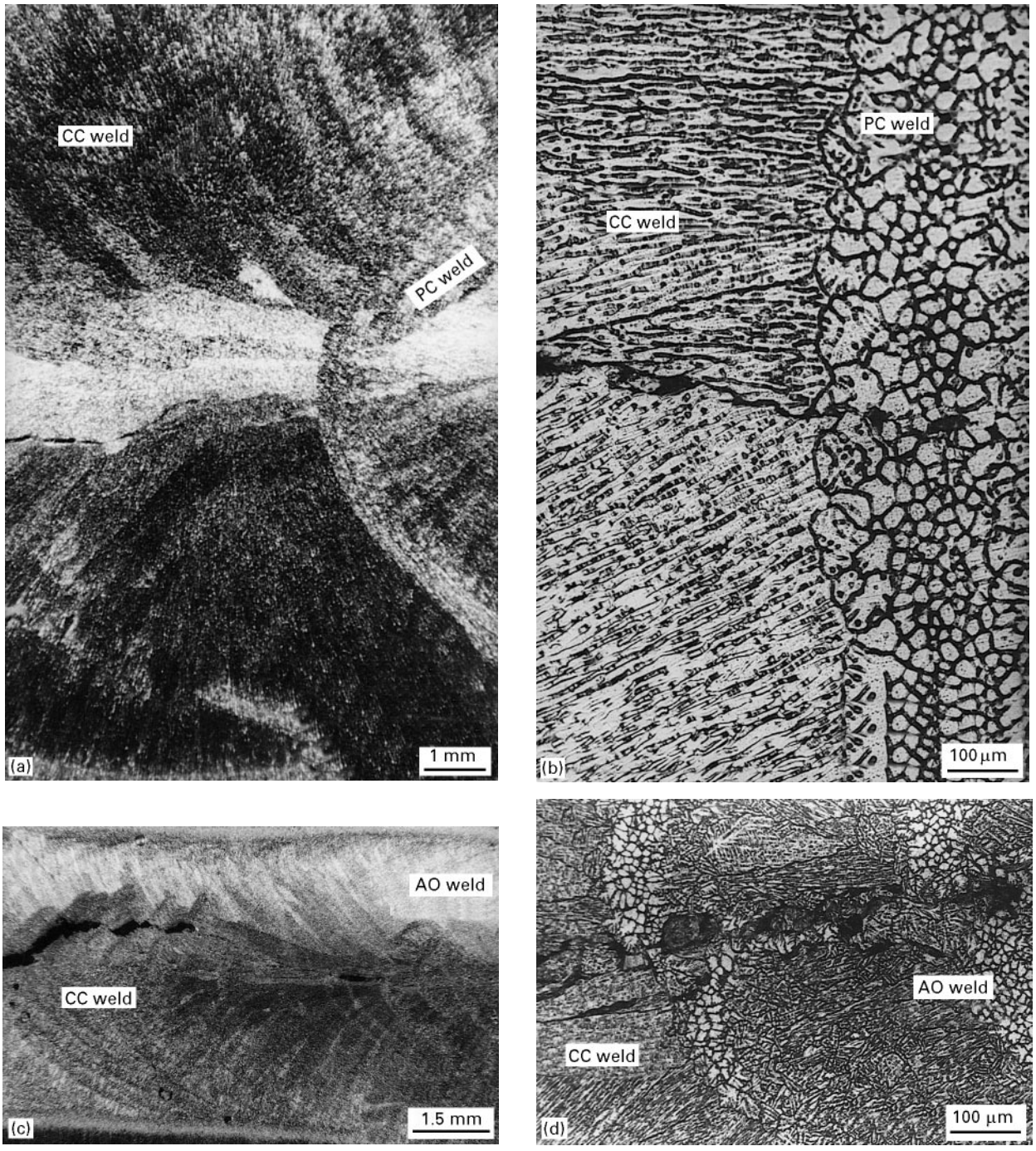

Figure 13 (a) Macrostructure of the area where switch-over from continuous to pulsed current was introduced showing crack arrest, (b) columnar-to-equiaxed transition in microstructure near the crack arrest zone shown in (a), (c) macrostructure of the area where arc oscillation was introduced during continuous current welding showing crack arrest, and (d) columnar-to-equiaxed transition in microstructure near the crack arrest zone shown in (c).

additional growth centres. Fluid flow is also known to be present in PC welds due to periodic variation in the arc current (and therefore the arc pressure) [18]. This results in a transition from columnar to equiaxed grain structure as seen in Figs 4–6 and 8. The fluid flow may also change the growth rate of the solid–liquid interface periodically, leading to banding in AO welds (Fig. 8).

Further, due to the ever changing direction of the maximum temperature gradient, the usual competitive growth mechanism that applies in the case of columnar dendritic growth may not be operative. Therefore, instead of a few (initially) favourably orientated grains growing over larger distances, newer and newer grains would be favourably orientated with respect to the instantaneous direction of the maximum thermal gradient and would cease to be favourably orientated after growing over a short distance thus resulting in a smaller grain aspect ratio.

4.2. Hot cracking

As seen in Section 4.1., in CC welds, columnar grains from the opposite sides meet at the weld centre line, creating a plane of weakness. This explains why the hot cracks were preferentially orientated along the

TABLE IV Tensile properties of longitudinal (all weld) test samples (as-welded condition)

Condition	0.2% yield stress[a] (MPa)	Ultimate tensile stress (MPa)	Elongation (%)[b]
CC weld	190	250	1.4
PC weld	260	350	6.5
AO weld	210	360	10.0
Base metal (T81)	390	450	7.5

[a] 0.2% yield stress based on 25 mm gauge length.
[b] Elongation based on 25 mm gauge length.

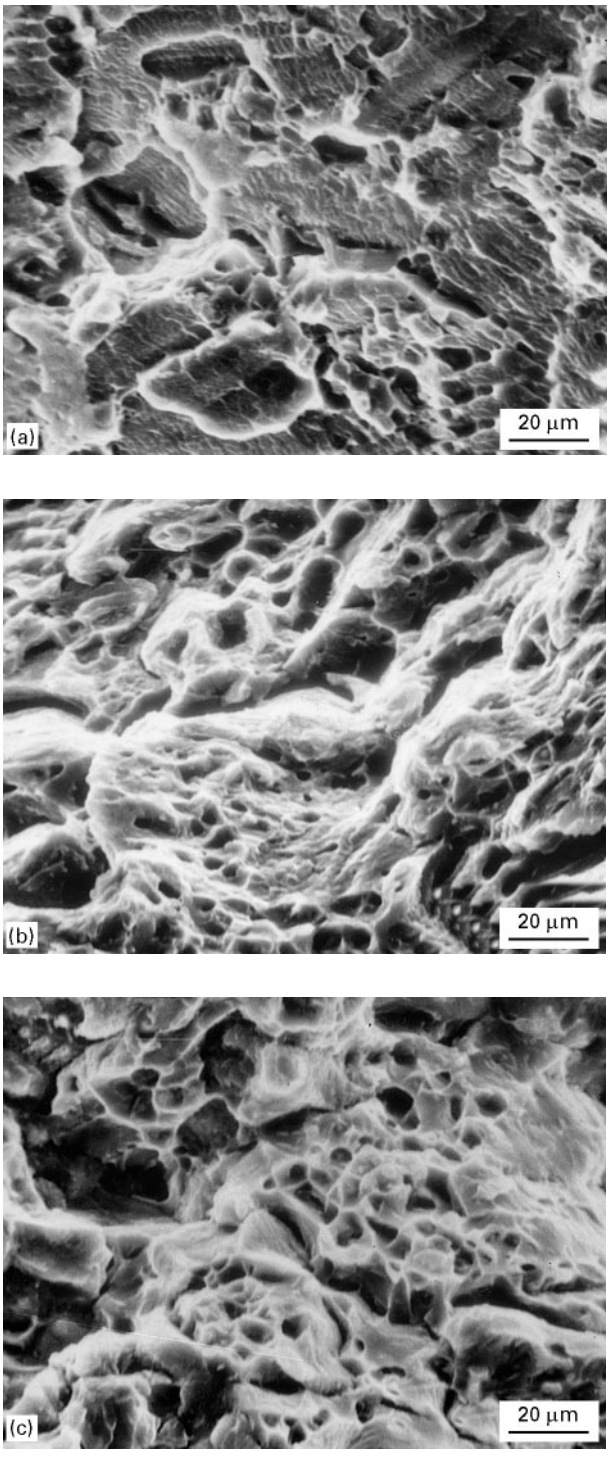

Figure 14 Tensile fracture surfaces in all-weld samples: (a) continuous current weld, (b) pulsed current weld, and (c) arc oscillation weld.

centre line of the continuous current welds. The welds made under PC and AO conditions were seen to have equiaxed grain structure in the zone near the weld centre line. It is well known that an equiaxed grain structure in solidifying alloys is more resistant to hot cracking than coarse columnar structures because of increased tortuosity of the crack path, improved grain contact due to the increase in the grain boundary area over which the last liquid to solidify distributes, etc. [19]. This explains the observed phenomenon of the termination of hot cracking (Fig. 13) upon switching from CC to PC or AO welding.

4.3. Tensile properties

Improvements in the tensile strength and ductility in PC and AO welds over CC welds could be attributed to microstructural refinement, i.e. finer grain size, smaller segregation distance and smaller size of secondary phases observed in PC and AO welds compared with CC welds. The fractographic observations are consistent with microstructures and ductility values obtained. It is evident from the present study that many improvements in the weld bead soundness, microstructure and properties are possible through modifications in the welding conditions, such as current pulsation and arc oscillation.

5. Conclusions

Aluminium–lithium alloy 1441 was shown to be weldable under AC GTA welding. Transition from columnar to equiaxed grain structure, reduction in weld metal cracking and improvement in weld tensile properties were achieved by introducing either pulsed current or arc oscillation conditions. The presence of a chill zone was shown, for the first time, in weld bead microstructures.

Acknowledgements

The authors would like to thank Mr S.L.N. Acharyulu, Director, DMRL, Dr C.R. Chakravorty, Dr D. Banerjee and Mr K. Mallikarjuna Rao for their continued encouragement and permission to publish this work. The authors appreciate the support of M/s. N. Viswanathan and S.P. Narsinga Rao, DRDL for welding trials with arc oscillation and Mr V.V. Rama Rao, DMRL for EMPA of the weldments. Support from the Kamensk-Uralsky Plant in producing the alloys is gratefully acknowledged.

Reference

1. A. A. GOKHALE, K. SATHYA PRASAD, V. KUMAR, C. R. CHAKRAVORTY, L. N. LESCHINER, S. M. MOZHAROVSKY and I. N. FRIDLYANDER, in "Aluminium alloys: their physical and mechanical properties" (Proceedings of the International Conference on Aluminium Alloys IV), edited by T. H. Sanders, Jr and E. A. Starke, Jr, September 1994, p. 428.
2. J. R. PICKENS, *J. Mater. Sci.* **20** (1985) 4247.
3. G. MADHUSUDHAN REDDY and A. A. GOKHALE, *Trans. Indian Inst. Met.* **46** (1993) 21.

4. M. F. GITTOS, "Gas shielded arc welding of the aluminium–lithium alloy 8090" Report 794401/556.2 (Welding Institute, London, 1987).
5. F. MATSUDA, K. NAKATA, Y. MIYANAYA, T. KAYANA and K. TSUKAMOTA, *Trans. Jap. Weld. Res. Inst.* **7** (1978) 33.
6. A. A. GOKHALE, G. M. ECER, A. A. TZAVARAS and H. D. BRODY, "Grain refinement in castings and welds", edited by G. Abbaschian and S. A. David (The Metallurgical Society, Warrandale, PA, 1982) p. 223.
7. J. E. RAMIREZ, B. HAN, and S. LIU, *Metall. Mater. Trans. A* **25A** (1994) 2285.
8. F. MATSUDA, K. NAKATA and R. AYANI, *Trans. Jap. Weld. Res. Inst.* **12** (1993) 93.
9. G. J. DAVIES and G. GARLAND, *Int. Metall. Rev.* **20** (1975) 83.
10. G. J. GARLAND, *Metal Construction & Brit. Welding J.* **4** (1974) 121.
11. F. MATSUDA, H. NAKAGAWA, K. NAKATA and R. AYANI, *Trans. Jap. Weld. Res. Inst.* **7** (1978) 111.
12. B. P. PEARCE and H. W. KERR, *Metall. Trans* **2B** (1981) 479.
13. S. KOU and Y. LE, *ibid.* **16A** (1985) 1887.
14. *Idem*, *Welding J.* **65** (1986) 314s.
15. T. GANAHA, B. P. PEARCE and H. W. KERR, *Metall. Trans.* **11A** (1980) 1351.
16. S. SRIRAM, G. B. VISWANATHAN, K. S. PRASAD, A. GOKHALE, D. BANERJEE and R. SIVAKUMAR, in Proceedings of the Conference on Metastable Microstructures, edited by D. Banerjee and L. A. Jacobson, (New Delhi, 1993) p. 103.
17. H. W. KERR and J. C. VILLAFUERTE, in "The metal science of joining", edited by M. J. Cieslak, J. H. Perepezko, S. Kang and M. E. Glicksman, (The Metallurgical Society, Warrandale, PA, 1992) p. 11.
18. G. M. ECER, A. TZAVARAS, A. A. GOKHALE and H. D. BRODY, in Proceedings of the Trends in Welding Research in the United States, Louisiana, November 1981, edited by S. A. David (American Society for Metals, Metals Park, OH) p. 419.
19. M. C. FLEMINGS, " Solidification processing" (McGraw-Hill, New York, 1974) p. 255.

Received 13 November 1995
and accepted 10 February 1997